Chemogenomic Screen for Imipenem Resistance in Gram-Negative Bacteria

Jessica Y. El Khoury,[a] Alexandra Maure,[a] Hélène Gingras,[a] Philippe Leprohon,[a] Marc Ouellette[a]

[a]Axe des Maladies Infectieuses et Immunitaires du Centre de Recherche du CHU de Québec and Département de Microbiologie, Infectiologie et Immunologie, Faculté de Médecine, Université Laval, Québec, Québec, Canada

ABSTRACT Carbapenem-resistant Gram-negative bacteria are considered a major threat to global health. Imipenem (IMP) is used as a last line of treatment against these pathogens, but its efficacy is diminished by the emergence of resistance. We applied a whole-genome screen in *Escherichia coli*, *Klebsiella pneumoniae*, and *Pseudomonas aeruginosa* isolates that were submitted to chemical mutagenesis, selected for IMP resistance, and characterized by next-generation sequencing. A comparative analysis of IMP-resistant clones showed that most of the highly mutated genes shared by the three species encoded proteins involved in transcription or signal transduction. Of these, the *rpoD* gene was one of the most prevalent and an *E. coli* strain disrupted for *rpoD* displayed a 4-fold increase in resistance to IMP. *E. coli* and *K. pneumoniae* also specifically shared several mutated genes, most involved in membrane/cell envelope biogenesis, and the contribution in IMP susceptibility was experimentally proven for amidases, transferases, and transglycosidases. *P. aeruginosa* differed from the two *Enterobacteriaceae* isolates with two different resistance mechanisms, with one involving mutations in the *oprD* porin or, alternatively, in two-component systems. Our chemogenomic screen performed with the three species has highlighted shared and species-specific responses to IMP.

IMPORTANCE Gram-negative carbapenem-resistant bacteria are a major threat to global health. The use of genome-wide screening approaches to probe for genes or mutations enabling resistance can lead to identification of molecular markers for diagnostics applications. We describe an approach called Mut-Seq that couples chemical mutagenesis and next-generation sequencing for studying resistance to imipenem in the Gram-negative bacteria *Escherichia coli*, *Klebsiella pneumoniae*, and *Pseudomonas aeruginosa*. The use of this approach highlighted shared and species-specific responses, and the role in resistance of a number of genes involved in membrane biogenesis, transcription, and signal transduction was functionally validated. Interestingly, some of the genes identified were previously considered promising therapeutic targets. Our genome-wide screen has the potential to be extended outside drug resistance studies and expanded to other organisms.

KEYWORDS chemical mutagenesis, carbapenem resistance, *Escherichia coli*, *Klebsiella pneumoniae*, *Pseudomonas aeruginosa*

T he World Health Organization (WHO) refers to antimicrobial resistance (AMR) as a major threat to global health and has established a list of priority pathogens for research and development of new effective antibiotics (1). Among the urgent threats is carbapenem resistance in the Gram-negative species *Escherichia coli* and *Klebsiella pneumoniae*. Both are commensal bacteria of the gastrointestinal tract of human and animals; they harbor many virulence factors and are responsible for different types of infections (2, 3). Another threat is represented by the opportunistic pathogen *Pseu-*

domonas aeruginosa (4). Those three bacterial species are leading causes of hospital-acquired infections (5).

Carbapenems such as imipenem (IMP) and meropenem (MEM) are β-lactam antibiotics (6) that bind and inhibit multiple penicillin binding proteins (PBPs) while resisting hydrolysis by class A extended-spectrum β-lactamases and class C β-lactamases (AmpC) (7). Carbapenems are used as a last line of treatment against multidrug-resistant Gram-negative pathogens (7). Nonetheless, resistance against carbapenems has been detected in *Enterobacteriaceae* mainly due to the production of more-potent β-lactamases such as *K. pneumoniae* carbapenemases (KPCs), class B metallo-β-lactamases (e.g., VIM, NDM, and IMP) and class D (OXA-type) β-lactamases found both on plasmids and in the chromosome (2, 8). Resistance resulting from the loss or modification of porins (OmpK35/36 for *K. pneumoniae* and OmpC/F for *E. coli*), in combination with the production of plasmid-encoded or chromosomally encoded AmpC, was also observed (9–12). The loss of the porin OprD in *P. aeruginosa* constitutes the major driver of carbapenem resistance, although resistance due to class B metallo-β-lactamases was also reported (13–16). β-lactam and β-lactamase inhibitor combinations (e.g., IMP-relebactam, MEM-vaborbactam) are showing promising results *in vitro* and in clinical trials against carbapenem-resistant Gram-negative bacteria (7, 17, 18). Both IMP and MEM target PBPs, and usually high-level resistance to IMP correlates with decreased susceptibility to MEM (19, 20). Studies performed with IMP have been useful for understanding the mode of action and resistance to carbapenems.

Exploring resistance to antibiotics at the genomic level is proving useful at revealing drug targets and modes of action, resistance mechanisms, and genes or mechanisms that play subtler roles such as facilitating resistance or compensating for fitness cost (21–24). The objective of this study was to apply a whole-genome sequencing (WGS) screen for IMP resistance in sensitive isolates of *E. coli*, *K. pneumoniae*, and *P. aeruginosa*. This screen couples chemical mutagenesis, selection for IMP resistance, and the characterization of IMP-resistant clones by next-generation sequencing (NGS). This approach, called "Mut-Seq" (25), has been helpful for various studies, including studies of drug resistance (26, 27). We found that the *rpoD* gene, encoding an RNA polymerase sigma factor, was the most prevalent mutated gene among IMP-resistant clones from the three species, and we experimentally validated its role in IMP resistance in *E. coli*. Mutations were also detected in several genes related to the cell wall and membrane biogenesis, and these are shown to confer low-level IMP resistance in *Enterobacteriaceae*. Finally, mutations in OprD were frequent in *P. aeruginosa* but we show that two-component (TC) signal transduction systems are also likely involved in IMP resistance.

RESULTS

Chemical mutagenesis and selection for resistance to IMP. *E. coli* ATCC 25922, *K. pneumoniae* ATCC 13883, and *P. aeruginosa* ATCC 27853 were treated with ethyl methane sulfonate (EMS) and selected for growth in the presence of IMP. The EMS concentrations and exposure and recovery times as well as the IMP concentrations for selection were optimized (see Materials and Methods). The minimum concentration of IMP used for selection was determined as the concentration at which growth occurred in the presence of IMP for the mutagenized populations but not for the nonmutagenized control populations.

The IMP-resistant clones for the three species were between 2-fold and 16-fold more resistant than the respective parental wild-type (WT) clones (Tables 1 and 2; see also Table S1 in the supplemental material). The levels of resistance to IMP measured for most clones of *E. coli* and *K. pneumoniae* were considered intermediate (MIC, 2 μg/ml) according to the Clinical and Laboratory Standards Institute (CLSI) guidelines (28). The IMP MIC for two *E. coli* clones and five *K. pneumoniae* clones was 4 μg/ml, a level consistent with clinical resistance (Table 1 and Table S1, respectively). According to the MIC breakpoints for *P. aeruginosa*, all but one clone reached resistance levels consistent with clinical resistance (MIC, ≥8 μg/ml) (Table 2). We observed that cells with higher

TABLE 1 IMP MICs for *E. coli* ATCC 25922 mutants and amino acid substitutions detected in genes mutated in at least three mutants

Strain[a]	IMP MIC (µg/ml)[b]	Gene ID and mutation[c]												
		DR76 3827 (yceG)	DR76 2948	DR76 1787 (amiC)	DR76 1419 (rpoD)	DR76 3839 (rne)	DR76 3362	DR76 1882 (nlpD)	DR76 689 (wecA)	DR76 475	DR76 727 (gidA)	DR76 4272 (tolA)	DR76 2503 (slt)	DR76 839 (spoT)
WT	0.25													
M27	0.5							G163D						
M38	0.5		P380L											
M5	1	A212T		G402R										
M6	1		P380L		A72V									
M7	1	Y274H		**P380L**										
M10	1					Q705*								
M16	1													
M17	1							276 Ins						
M18	1													
M19	1					R335C								
M20	1			**G402R**							**A539V**			
M24	1		P380L	A203T								A223T		
M25	1		P380L	E229K							A77T			
M28	1	W162*												
M33	1	S230L								A122V			121 ins	
M39	1		P380L	G197S										
M40	1		P380L											
M42	1													
M44	1						D113N		P101S					
M46	1		P380L											
M49	1		P380L					D321G						
M50	1	P281S	P380L	Q353*										
M1	2	E224K				Q692*								
M2	2	M1I									**A254V**			
M3	2	T273I				**Q775***								
M4	2				A444V		D318A		G45R					
M8	2		P380L										W455*	
M9	2							276 Ins						
M11	2	W156*				P250L Q691*					**M67I**			
M12	2				A444T				**R40C**					
M13	2				I457L				D159N					
M15	2	**Q92***												
M21	2										R204C			
M22	2		P380L					342 Del						
M23	2		D376N		**A444V**									
M29	2	P246L					**A429T**							
M30	2	T273I												
M31	2	289 Ins												
M32	2	Q92*												P168S
M34	2	P246L					A429T							
M35	2	W24*				Q649*								
M36	2						D113N		P101S					
M37	2	W193*							A149V					
M41	2			Q57*										
M43	2				A444V									
M45	2			R102C	A444V							G316E		
M47	2	Q92*									V102M			
M48	2	E107K					A259V		**Q161***					
M14	4	S230L	P380L	Q15*									**R475***	**A138V**
M26	4				A444T				G51E					

[a]Mutants are listed in ascending order of IMP MIC.

[b]MICs were monitored with at least three biological replicates. For all differences of 2-fold or higher, there was no variability in the observed MICs.

[c]Mutations correspond to amino acid substitutions, and numbers refer to amino acid positions in the protein. In the case of small insertions (Ins) or deletions (Del), the number indicated refers to the nucleotide position at which these occurred in the gene. Asterisks denote stop codons. ID, identifier. Mutations indicated in bold have been functionally tested for their role in IMP resistance by individual transformation in *E. coli* ATCC 25922 (see Table 5).

IMP MICs also showed decreased susceptibilities to MEM (Table 3). The MEM MICs increased by 2-fold, 4-fold, and up to 16-fold in IMP-selected *K. pneumoniae*, *E. coli*, and *P. aeruginosa*, respectively (Table 3). The MEM resistance in *P. aeruginosa* reached levels consistent with clinical resistance.

TABLE 2 IMP MICs for *P. aeruginosa* ATCC 27853 mutants and amino acid substitutions detected in genes mutated in two or more mutants

Strain[a]	IMP MIC (µg/ml)[b]	Gene ID[c]				
		A4W92_06800 (oprD)	A4W92_13070 (sensor HK)[d]	A4W92_13065 (response regulator)	A4W92_04840 (sensor HK)[d]	A4W92_05675 (phoQ)
WT	2					
M2	4	G183D				
M44	8	S325F				
M13	8	G402D				
M31	8			A174V		
M35	8			A174V		
M40	8			A174V		
M47	8			M53V		
M36	8					E198K
M8	8		A252V			
M39	8		A252V			
M23	8		G260D			
M30	8		G260D			
M43	8		G260D			
M37	8		V268M			
M28	8		S285F			
M25	8		L303F			
M1	8		R419H			
M3	8		R419H			
M11	16		R419H			
M5	16		A252V			Q258*
M12	16		E291K			
M14	16		E291K			
M16	16		E291K			
M6	16				R419H	
M9	16				R419H	
M4	16	W6*				
M10	16	W6*				
M18	16	W6*				
M22	16	W6*				
M33	16	W6*				
M26	16	Q19*				
M32	16	Q19*				
M29	16	Q30*				
M17	16	W65*				
M20	16	Q67*				
M48	16	Q67*				
M38	16	Q79*				
M24	16	W138*				
M27	16	W138*				
M45	16	W138*				
M46	16	W138*				
M7	16	Q158*				
M50	16	Q158*				
M42	16	Q235*				
M21	16	W277*				
M41	16	Q295*				
M19	16	Q296*				
M15	16	W339*				
M34	16	Y343N				
M49	16	W415*				

[a]Mutants are listed in ascending order of IMP MIC and grouped by mutation profiles.
[b]MICs were monitored with at least three biological replicates. For all differences of 2-fold or higher, there was no variability in the observed MICs.
[c]Mutations correspond to amino acid substitutions, and numbers refer to amino acid position in the protein. Asterisks denote stop codons.
[d]HK, histidine kinase.

Clusters of orthologous groups of mutated proteins. The genomes of 145 IMP-resistant clones (45 *K. pneumoniae*, 50 *E. coli*, and 50 *P. aeruginosa* clones) were analyzed by NGS. The genomes of the parent WT strains were also sequenced. A total of 3,810 single nucleotide (nt) variants (SNVs) were identified in the *E. coli* mutants (Fig. 1A), with a majority of the clones having at least 40 SNVs (Table S2). In *K.*

TABLE 3 IMP and MEM MICs for some selected mutants of *E. coli*, *K. pneumoniae*, and *P. aeruginosa*

Strain	MIC (μg/ml)[a]	
	IMP	MEM
E. coli		
ATCC 25922	0.25	0.03
M11	2	0.03
M14	4	0.12
M23	2	0.06
M26	4	0.12
K. pneumoniae		
ATCC 13883	1	0.06
M6	4	0.12
M9	4	0.12
M17	2	0.06
M18	2	0.12
M21	2	0.06
M40	2	0.06
P. aeruginosa		
ATCC 27853	2	0.5
M2	4	2
M4	16	8
M5	16	8
M6	16	4
M31	8	2
M34	16	4
M36	8	4
M37	8	2

[a]MICs were monitored with at least three biological replicates. For all differences of 2-fold or higher, there was no variability in the observed MICs.

pneumoniae, 1,379 SNVs were detected (Fig. 1A), with an average of 22 mutations (range, 5 to 39) per genome (Table S3). In *P. aeruginosa*, 654 SNVs were identified (Fig. 1A), with an average of 10 mutations (range, 2 to 18) found per mutant (Table S4). SNVs were more prevalent in coding regions than in intergenic regions for all species, and nonsynonymous SNVs predominated among coding mutations (Fig. 1A). While we cannot exclude the possibility that some SNVs resulted from IMP selection alone, it is highly likely that most were instead genuinely induced by EMS treatment. First, resistant clones were obtained using experimental conditions optimized such that no clone would grow upon IMP selection if the culture was not initially mutagenized by EMS. Second, most SNVs consisted of G-to-A and C-to-T transitions (Fig. 1B), which is consistent with the mode of action of EMS (29), and these were widespread among the 145 mutants sequenced. Some small insertions and deletions (InDels) were also observed in coding regions, and these were more frequent in *P. aeruginosa* than in *E. coli* or *K. pneumoniae* (Fig. 1A).

We hypothesized that functional recurrence among mutated genes between species or clones would help in pinpointing the mutations that are the most relevant to IMP resistance. To ease comparisons among the three species, we relied classification using the Clusters of Orthologous Groups of proteins (COGs). The COG database is composed of over 4,600 specific functional COG descriptions grouped into 26 general category letter associations (30). We initially focused on the part of the COG descriptions corresponding to the mutated genes common to the three species, then on those shared by at least two species, and finally on the genes that are species specific but that were mutated in a higher number of clones. Thirty-five functional COG descriptions were found in common among the three species (Table S5). A third of these belonged to two general categories: (i) transcription mechanisms (K) and (ii) signal transduction mechanisms (T) (Fig. 2). The *rpoD* gene was the most prevalent in the COG category transcription, with mutations detected in a total of 10 mutants in the three species
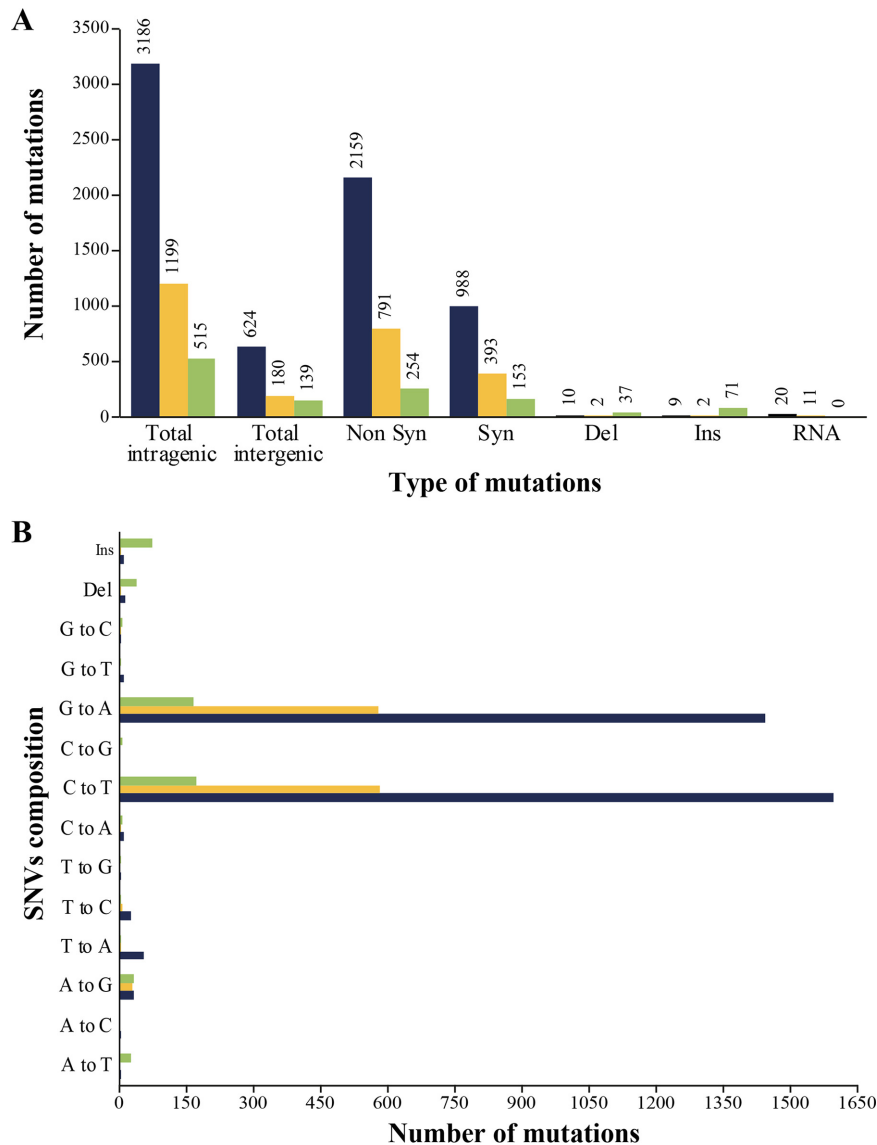
FIG 1 Summary of number and type of mutations induced by EMS in the three bacterial species. (A and B) Number and type (A) as well as distribution (B) of mutations found in Mut-Seq mutants selected for IMP resistance in *E. coli* (blue), *K. pneumoniae* (orange), and *P. aeruginosa* (green). Syn, synonymous; Non Syn, nonsynonymous; Del, deletion; Ins, insertion; RNA, rRNA, tRNA, transfer-messenger RNA (tmRNA), and noncoding RNA (ncRNA) (inclusive); SNV, single nucleotide variant.

(Table S5). A C58T transition occurred in *rpoD* for one mutant each of *K. pneumoniae* and *P. aeruginosa*, leading to G20S and E20K amino acid substitutions, respectively, while eight *E. coli* mutants harbored mutations leading to an A72V, A444V, A444T, or I457L substitution (Fig. 3A). Additional genes coding for DNA-binding transcriptional regulators, sensor histidine kinases (HK), major facilitator superfamily transporters, and multidrug transporters were also mutated in the three species, but the mutations were often seen in a single mutant for each species and thus they were not further studied (Table S5).

The *E. coli* and *K. pneumoniae* mutants shared 275 COG descriptions. Of these, 11 consisted of one-to-one matches of *E. coli* and *K. pneumoniae* proteins that shared at least 70% sequence identity (implying genuine functional similarity) and that were also mutated in at least two mutants in each species (Table 4). These 11 genes belonged to 7 general functional categories, the cell wall/membrane/envelope biogenesis category (M) being the most prevalent, with 4 mutated genes (Table 4). One of the 11 genes was
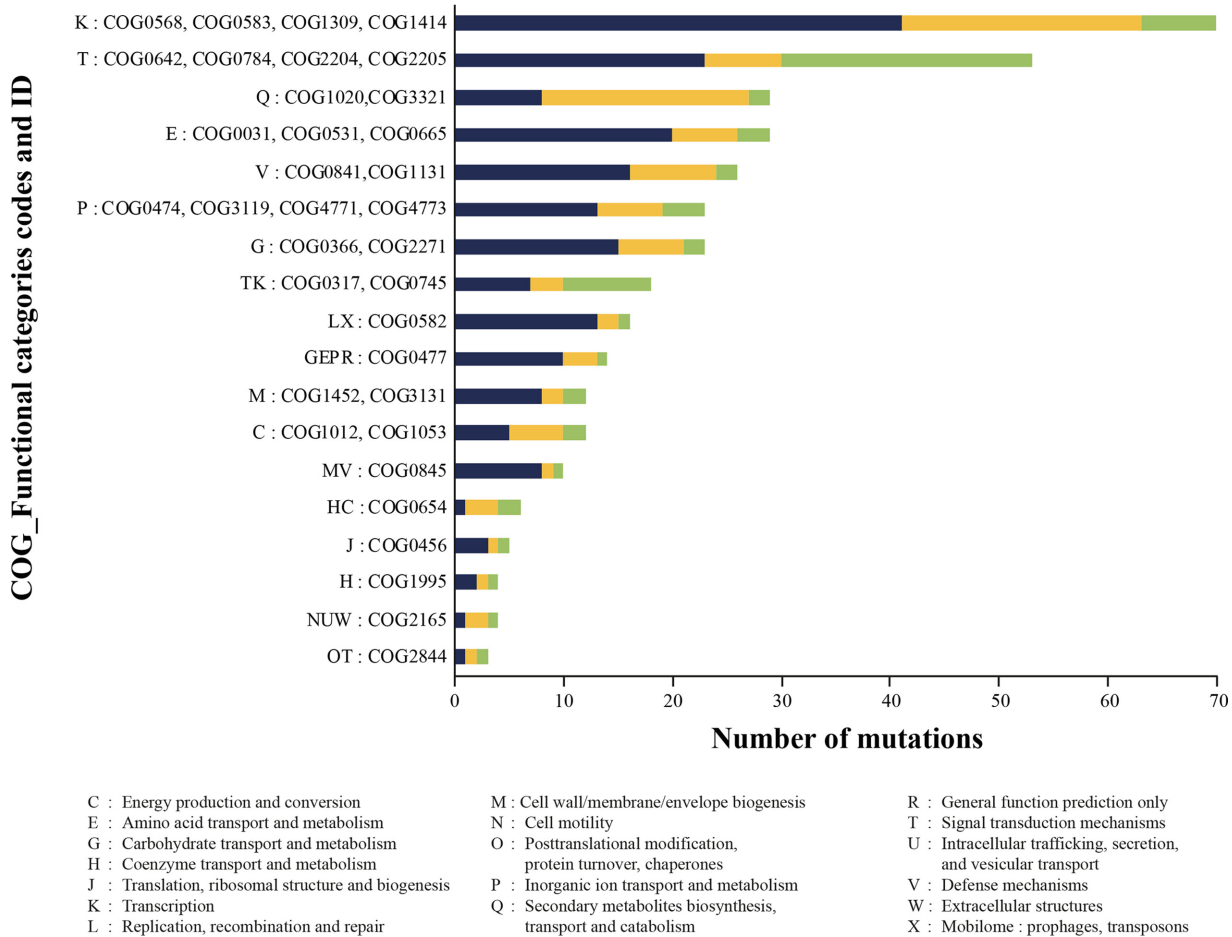
FIG 2 COG functional categories detected among the three species for the mutated genes. Mutated genes were classified into the appropriate COG, and the most common COGs shared by *E. coli* (blue), *K. pneumoniae* (orange), and *P. aeruginosa* (green) are shown.

amiC coding for an *N*-acetylmuramoyl-ʟ-alanine amidase mutated in 9 *E. coli* and 26 *K. pneumoniae* mutants (Table 4). A majority of mutations localized to the AmiC domain of the protein, and several were nonsense mutations (see Fig. S1A in the supplemental material). Another gene was *nlpD*, mutated in 5 *E. coli* and 18 *K. pneumoniae* mutants (Table 4). This gene codes for the activator of AmiC (31). Similarly to *amiC*, several nonsense mutations were observed in *nlpD* (Fig. S1B). The third gene was *wecA*, coding for an undecaprenyl-phosphate alpha-*N*-acetylglucosaminyl 1-phosphate transferase mutated in 5 mutants of each species (Table 4). The last gene from the M category was *slt*, which codes for a soluble lytic murein transglycosylase. The *slt* gene was mutated in 5 mutants, a majority harboring nonsense mutations (Fig. S1C). The remaining 7 genes were not part of the cell wall biogenesis category and had unrelated functions (Table 4). These were shared by 4 to 9 *E. coli* and *K. pneumoniae* mutants (Table 4). For gene *clbJ* (COG1020, category Q), the E1684G mutation found in 15 mutants of *K. pneumoniae* was present also in the IMP-sensitive *E. coli* WT strain, making it less likely to contribute to IMP resistance.

P. aeruginosa mutants were fairly distinct compared to *E. coli* and *K. pneumoniae* mutants, and these were thus not directly compared to *E. coli* and *K. pneumoniae* mutants in 2-way comparisons.

Species-specific mutations. Recurrence among clones was previously shown to ease the identification of SNVs contributing to the resistance phenotype (26), so, to retrieve gene candidates specifically mutated in *E. coli*, we thus focused on those mutated in at least 3 clones (Table 1). The gene *yceG* encoding a cell division protein
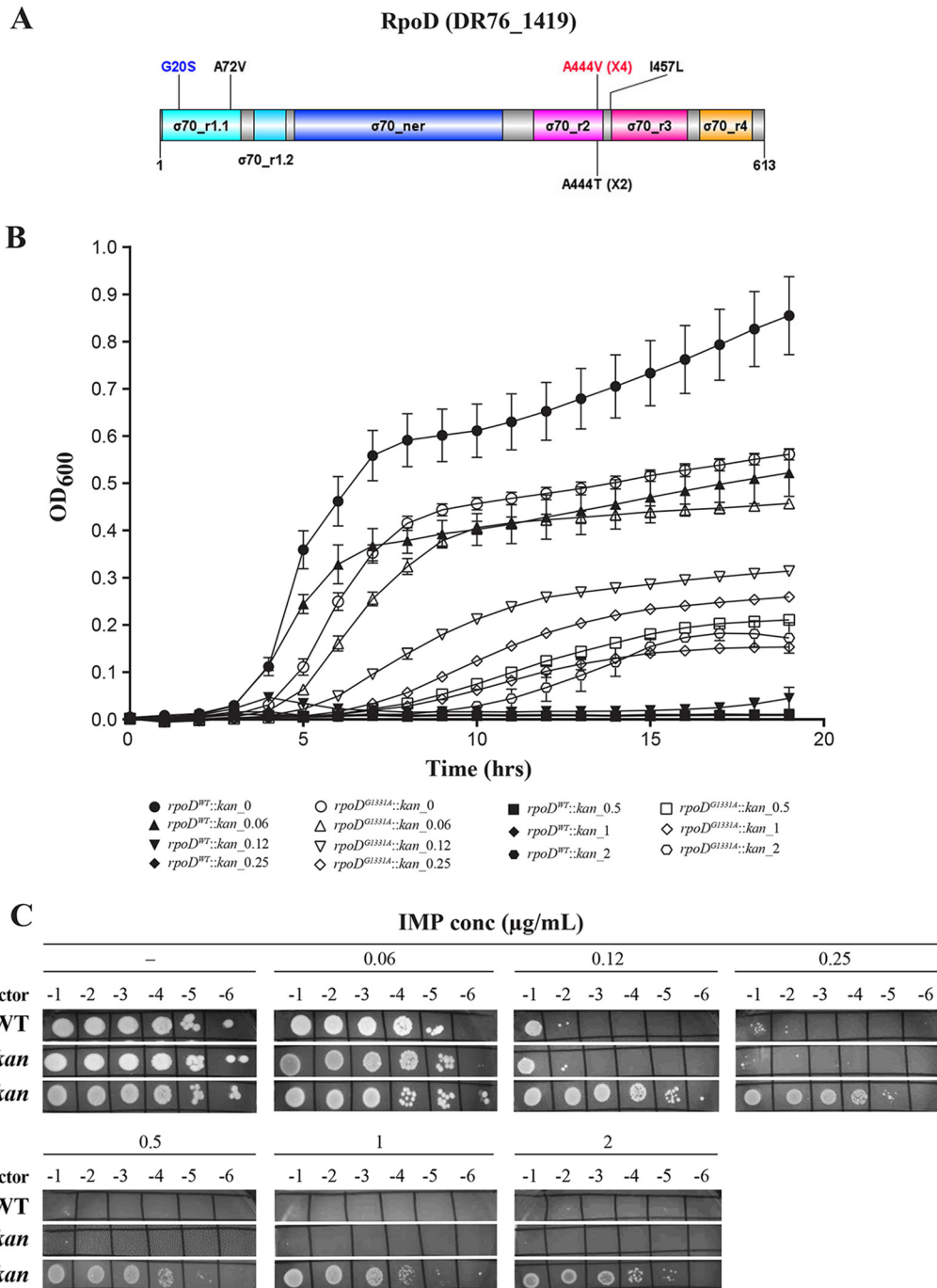
FIG 3 Validation of the role of RpoD in IMP susceptibility. (A) Schematic representation of the RpoD (DR76_1419) domains. The mutation marked in red was used to generate the single knock-in in *E. coli* ATCC 25922 (*rpoD*^{G1331A}::*kan*). Numbers between parentheses indicate the recurrence of the mutation among clones. The G20S and E20K (not shown) substitutions were found in only one mutant of *K. pneumoniae* and one of *P. aeruginosa*, respectively. σ70_r, sigma 70_region; ner, nonessential region. (B) Growth curves of *rpoD*^{WT}::*kan* and *rpoD*^{G1331A}::*kan* in LB in the absence or presence of IMP at the indicated concentrations. Data shown represent averages ± standard errors of the means (SEM) of results from three biological replicates done in technical triplicate. (C) Cultures of *E. coli* ATCC 25922 WT, *rpoD*^{WT}::*kan*, and *rpoD*^{G1331A}::*kan* were serially diluted and spotted on LB agar plates in the absence (-) or presence of imipenem (IMP) at the indicated concentrations. Plates were incubated overnight at 37°C and photographed. Data shown are representative of results from three biological replicates.

was the most prevalent among *E. coli* clones, with 15 SNVs (including 5 nonsense mutations) detected in 20 mutants (Table 1). The second most prevalent gene was DR76_2948 coding for a trehalose-6-phosphate synthase, with two mutations (D376N and P380L) found in a total of 14 *E. coli* mutants (Table 1). Seven different mutations (5

TABLE 4 COG categories and functional descriptions of genes mutated in at least two mutants of *E. coli* and *K. pneumoniae*

COG category	COG description	Function	Gene ID[a] E. coli[b,c]	K. pneumoniae[b]	Gene designation[b]
C	COG4656	Na⁺-translocating ferredoxin:NAD⁺ oxidoreductase Rnf	**DR76_3209** (2)	**DR88_4075** (2)	*rnfC*
G	COG2814	Predicted arabinose efflux permease	DR76_1590 (2)		*nanT*
			DR76_1762 (2)		
			DR76_4561 (2)		*araJ*
				DR88_690 (3)	
J	COG0445	tRNA U34 5-carboxymethylaminomethy modifying enzyme MnmG/GidA	***DR76_727*** (4)	**DR88_3339** (2)	*gidA*
	COG0215	Cysteinyl-tRNA synthetase	**DR76_4436** (2)	**DR88_4524** (3)	*cysS*
L	COG0847	DNA polymerase III	DR76_3797 (2)	DR88_1301 (2)	
M	COG0860	N-acetylmuramoyl-L-alanine amidase	***DR76_1787*** (9)	**DR88_2369** (26)	*amiC*
	COG1388	LysM repeat	***DR76_1882*** (5)	**DR88_2261** (18)	*nlpD*
	COG0472	UDP-N-acetylmuramyl pentapeptide phosphotransferase/UDP-N-acetylglucosamine-1-phosphate transferase	***DR76_689*** (5)	**DR88_3479** (5)	*wecA*
	COG0741	Soluble lytic murein transglycosylase	***DR76_2503*** (3)	**DR88_109** (2)	*slt*
	COG0438	Glycosyltransferase involved in cell wall biosynthesis	DR76_4781 (3)		
			DR76_1541 (2)		
				DR88_1607 (3)	
NW	COG3188	Outer membrane usher protein FimD/PapC	DR76_1626 (2)		*papC*
			DR76_2428 (2)		*fimD*
			DR76_3348 (3)		*fimD*
			DR76_3932 (3)		*fimD*
				DR88_2135 (2)	*fimD*
				DR88_3815 (2)	
				DR88_397 (2)	*StfC*
P	COG4773	Outer membrane receptor for ferric coprogen and ferric-rhodotorulic acid	DR76_3822 (2)		*fhuE*
				DR88_4364 (2)	
Q	COG1020	Nonribosomal peptide synthetase component F	**DR76_2812** (2)	**DR88_1541** (15)	*clbJ*
R	COG2373	Uncharacterized conserved protein YfaS	**DR76_408** (2)	**DR88_2018** (2)	
	COG0612	Predicted Zn-dependent peptidase	DR76_3359 (3)	DR88_3068 (3)	
S	COG1649	Uncharacterized lipoprotein YddW	***DR76_3362*** (6)	**DR88_3813** (3)	
TK	COG0317	(p)ppGpp synthase/hydrolase	***DR76_839*** (2)	**DR88_3198** (2)	*spoT*
V	COG0841	Multidrug efflux pump subunit AcrB	DR76_4821 (7)		*MdtB*
			DR76_4822 (2)		*MdtC*
				DR88_665 (2)	
				DR88_584 (2)	*acrB*

[a]Gene accession numbers are indicated for *E. coli* ATCC 25922 and *K. pneumoniae* ATCC 13883. The number of mutants in which the genes were found mutated is indicated within parentheses.
[b]Gene designations in bold represent orthologues sharing at least 70% sequence identity at the protein level.
[c]Gene designations in italics represent genes that have been functionally tested for their role in resistance to IMP by individual transformation in *E. coli* ATCC 25922 WT (see Table 5).

of which were nonsense) occurred in the *rne* gene for six mutants. This gene codes for RNase E. Four different mutations occurred in five mutants for gene DR76_475, encoding a glutamate racemase. Finally, the *tolA* gene, which is part of the Tol-Pal cell envelope complex, was mutated in three *E. coli* mutants, including mutants M24 and M45, which also hold a mutated *amiC* gene (Table 1). A more exhaustive list of mutations can be found in Table S6.

The mutational landscape of *P. aeruginosa* was more limited than that determined for *E. coli* (Fig. 1A), so we lowered our cutoff for candidate genes to correspond to those mutated in at least two mutants (Table S7). All mutants had a mutation either in the porin OprD or in two-component systems (TCSs) consisting of a sensor HK and a response regulator (Table 2). For *oprD*, 20 different mutations were found in 28 *P. aeruginosa* clones, 16 of which led to a stop codon (Table 2). Every mutant with a nonsense mutation in *oprD* had an IMP MIC of 16 μg/ml, representing an 8-fold increase compared to WT *P. aeruginosa* (Table 2). This was also the case for mutant M34

TABLE 5 Functional validation of mutation detected in *E. coli* IMP-resistant mutants

Gene ID[a]	Gene designation	Source[b]	Mutation		MIC (μg/ml)[c]	
			Nucleotide	Amino acid	IMP	MEM
Single knock-in						
ATCC 25922					0.25	0.03
DR76_475		M2	G761A	A254V	0.25	ND
DR76_689	*wecA*	M12	G118A	R40C	0.25–0.5	ND
DR76_727	*gidA*	M20	C1616T	A539V	0.25	ND
DR76_839	*spoT*	M14	G413A	A138V	0.25–0.5	ND
DR76_1419e	*rpoD*	M23	G1331A	A444V	1	0.06
DR76_1787	*amiC*	M20	G1204A	G402R	0.5	0.03
DR76_1882	*nlpD*	M48	C481T	Q161*	0.5	0.03
DR76_2503	*slt*	M14	C1423T	R475*	0.5	0.03
DR76_2948		M50	C1139T	P380L	0.25	ND
DR76_3362		M29	G1285A	A429T	0.25	ND
DR76_3827	*yceG*	M15	G274A	Q92*	0.25	ND
DR76_3839	*rne*	M3	C2323T	Q775*	0.5	0.03
DR76_4272	*tolA*	M11	C201T	M67I	0.5	0.03
Double knock-in						
Gene 1						
amiC				G402R		
Gene 2						
slt				R475*	1	0.06
yceG				Q92*	0.5	ND
gidA				A539V	0.5	ND

[a]Single knock-in, mutations in genes were transformed in an individual fashion; Double knock-in, mutations in two genes were transformed into the same *E. coli* ATCC 25922 cells. Gene IDs in bold had mutations in at least two *E. coli* and *K. pneumoniae* mutants (see Table 4). The gene in italics was mutated in *E. coli*, *K. pneumoniae*, and *P. aeruginosa*.

[b]The mutant whose genomic DNA was used to amplify the mutation by PCR to generate the knock-in cassettes.

[c]MICs were monitored with at least three biological replicates. For all differences of 2-fold or higher, there was no variability in the observed MICs. The *kan* resistance marker was removed from all transformants using the FLP/FLPe recombinase except for *rpoD*. ND, not determined.

harboring a Y343N substitution in OprD, while other *oprD* coding mutations (G183D, G402D, and S325F) were associated with lower IMP resistance levels (Table 2). For TCSs, 15 mutants had a mutation in the sensor HK A4W92_13070 (Table 2). This HK is part of a two-component signal transduction system for which A4W92_13065, mutated in 4 independent *P. aeruginosa* clones (Table 2), is the response regulator. Interestingly, mutants M6 and M9 had a R419H mutation in the HK A4W92_04840 (Table 2), the same change that occurred in mutants M1, M3, and M11 for the HK described above (A4W92_13070). Lastly, the sensor HK PhoQ (A4W92_05675) was mutated in *P. aeruginosa* clones M5 (Q258*) and M36 (E198K) (Table 2).

Phenotypic validation of mutations highlighted by Mut-Seq. The role of specific mutations in resistance to IMP was tested in *E. coli* ATCC 25922 using a knock-in approach. This involved the transformation of WT cells with a DNA cassette made of a PCR fragment containing the mutation fused to a kanamycin (Kan) resistance gene flanked by FLP recombination target (FRT) sequences used for the removal of the selection marker by the FLP/FLPe recombinase. For the *rpoD* gene mutated in all species, we tested the G1331A transition that was detected in *E. coli* and that led to the A444V amino acid substitution (Table 5). This mutation conferred a 4-fold increase in IMP resistance in the *rpoD*^G1331A^::*kan* transformants compared to the *rpoD*^WT^::*kan* cells used as a control (we failed to remove the *kan* resistance marker in *rpoD*^G1331A^::*kan* despite several attempts) (Table 5). The transformant *rpoD*^WT^::*kan* had the same IMP MIC (0.25 μg/ml) as the *E. coli* ATCC 25922 WT. The A444V mutation allowed cells to sustain higher IMP concentrations than the control both in liquid medium (Fig. 3B) and on solid agar (Fig. 3C) but conferred a slight fitness cost in the absence of IMP (Fig. 3B). Interestingly, the *rpoD*^G1331A^::*kan* mutant had decreased susceptibility also for MEM (Table 5).
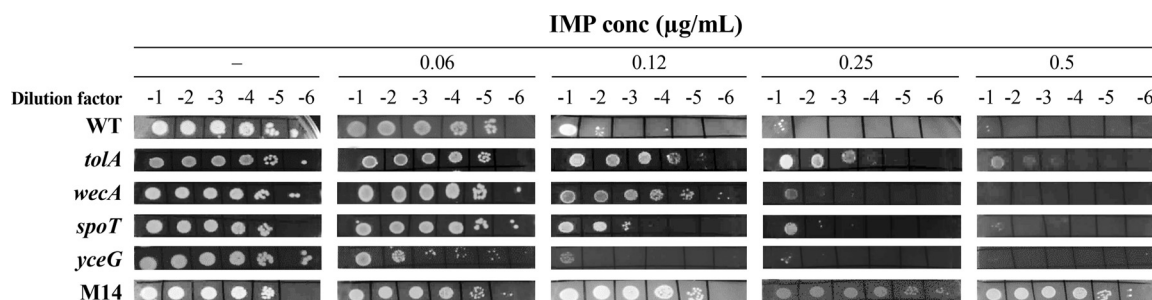
FIG 4 Validation of the roles of WecA and SpoT in IMP susceptibility in *E. coli*. Cultures of *E. coli* ATCC 25922 WT; of single knock-ins harboring TolA (M67I), WecA (R40C), SpoT (A138V), or YceG (Q92*) mutations; and of *E. coli* IMP-resistant mutant M14 were serially diluted and spotted on LB agar plates in the absence (-) or presence of imipenem (IMP) at the indicated concentrations. Plates were incubated overnight at 37°C and photographed.

Using the same knock-in approach, we also investigated the role in IMP resistance of mutations in genes shared by *E. coli* and *K. pneumoniae* mutants (Table 4). The G402R substitution in AmiC, a position mutated in two *E. coli* mutants and one mutant of *K. pneumoniae* (Fig. S1A), decreased the susceptibility to IMP by 2-fold when introduced into *E. coli* ATCC 25922 (Table 5). Similarly, the nonsense mutations Q161* and R475* in NlpD and Slt, respectively, increased the IMP MIC by 2-fold (Table 5). *E. coli* mutant M14 and *K. pneumoniae* mutant M17 had mutations in both *amiC* and *slt*, and the AmiC G402R and Slt R475* mutations were indeed additive in increasing the IMP MIC by 4-fold under conditions of cotransformation into *E. coli* ATCC 25922 (Table 5). This *amiC* and *slt* double knock-in also showed decreased susceptibility to MEM (Table 5). Despite being mutated in 5 mutants each of *E. coli* and *K. pneumoniae* (Table 4), the role of *wecA* mutations was less clear as the transformant for the R40C mutation (detected in *E. coli* mutant M12) was not conclusively altered for its IMP MIC (Table 5). Regarding the mutations in genes that are unrelated to cell wall biogenesis but that have at least 70% sequence identity between *E. coli* and *K. pneumoniae* (Table 4), we tested mutations A138V in SpoT, A429T in DR76_3362, and A539V in GidA, but, similarly to the results seen with *wecA*, none had a significant impact on the IMP MIC (Table 5).

We also tested some representatives of the most prevalent genes specifically detected in *E. coli*. The mutations in *yceG* and *rne* leading to the Q92* and Q775* nonsense mutations, respectively, as well as the P380L substitution in DR76_2948 and the M67I mutation in TolA, were independently transformed in *E. coli* ATCC 25922. The IMP MIC was increased by 2-fold (0.5 μg/ml) in the case of the *rne* and *tolA* knock-in (Table 5).

The knock-ins for mutations in *wecA* and *spoT* described above had an ambiguous phenotype by MIC measurements, so we looked for subtler phenotypes by monitoring their growth by serial dilution on solid medium in the presence of IMP. As expected, the *E. coli* M14 mutant (harboring an A138V mutation in SpoT) grew until it reached the highest cell dilution and IMP concentration tested. In contrast, *E. coli* ATCC 25922 WT grew only to the 10^{-1} dilution on an agar plate supplemented with 0.25 μg/ml of IMP (its MIC) (Fig. 4). As a positive control for transformation, we used the M67I mutation in TolA. This mutation allowed cells to grow until they reached the 10^{-2} dilution at 0.5 μg/ml (Fig. 4), consistent with the MIC of this transformant (Table 5). Mutations R40C in WecA and A138V in SpoT had an intermediate phenotype in growing with more dilutions than the WT cells at 0.12 μg/ml IMP and at the 10^{-1} dilution at 0.25 μg/ml IMP (Fig. 4). Given its recurrence, we also tested the *yceG* gene but the Q92* mutation did not increase growth in the presence of IMP and was even detrimental under the conditions tested (Fig. 4).

DISCUSSION

The use of whole-genome screens is now allowing holistic views of mechanisms of action and mechanisms of resistance against antimicrobial agents. We applied here a

Mut-Seq screen (25, 26, 32) combining chemical mutagenesis and NGS to obtain clones of *E. coli*, *K. pneumoniae*, and *P. aeruginosa* with decreased susceptibility to IMP. The main advantage of Mut-Seq in comparison to other approaches such as step-by-step drug selection is the rapidity with which resistant mutants are obtained (24 h versus months), hence accelerating studies on the mode of action or mechanisms of resistance to antimicrobials. We posited that using diverse species and analyzing a large set of independent mutants would pinpoint shared pathways of resistance as well as species-specific traits. As expected from phylogeny, the response of *E. coli* to IMP shared more similarity with *K. pneumoniae* than with *P. aeruginosa*. Some responses were shared among the three species, and while we concentrated on the genes mutated in the greatest number of mutants, it is quite possible that mutant-specific genes are also important for IMP responses.

The two main categories of orthologous proteins shared among the three species were those corresponding to transcription and signal transduction mechanisms. The most prevalent gene common to the three species was *rpoD*, which codes for the σ^{70} factor that is associated with the core RNA polymerase complex for initiation of specific transcription (33). Mutations in *rpoD* were in distinct domains, and we validated experimentally the role of the A444V substitution detected in several independent *E. coli* mutants. This substitution occurred in a region of RpoD that is highly conserved, as it is part of the −10 promoter recognition helix binding (34). One current limitation of our work is the lack of validation of the role of *rpoD* directly in *K. pneumoniae* or *P. aeruginosa*. This type of effort could form the basis of further studies. While *rpoD* has never been shown to be involved with IMP resistance, sigma factors are well known to regulate a number of genes often associated with responses to stress (35). Further work may also provide insights into the downstream target gene(s) responsible for the decrease in IMP susceptibility. Many other genes (62 in *E. coli* and 39 in *K. pneumoniae*), including several that are strain specific, that are involved in transcription were mutated, and some may indeed help in the response to IMP. Among many of the TCSs mutated in each of the three species, *evgS* and *phoQ* were common (see Table S5 in the supplemental material). Knock-in of *evgS* or *phoQ* was not possible because of the gene arrangement and the close proximity of their respective regulators *evgA* and *phoP*.

IMP inhibits bacterial cell wall synthesis by binding to and inactivating the PBPs, with the highest affinity to PBP-1a, PBP-1b, and PBP-2 (36, 37), leading to rapid cell lysis and death (38). MEM also targets PBPs, with the highest affinity for *Pseudomonas* PBP-2 and PBP-3. While less active than IMP against enterococci, it is more active against *P. aeruginosa* (39). Our highly IMP-resistant *P. aeruginosa* mutants and our *E. coli* knock-ins with at least 4-fold resistance to IMP were all less susceptible to MEM (Table 3 and Table 5), demonstrating that our findings with IMP can be applied to MEM as long as the IMP MIC has reached a minimum threshold. This corroborates results of other studies demonstrating that IMP-resistant *P. aeruginosa* strains are usually cross-resistant to MEM as well (19, 20). Similarly, *E. coli* strains selected for MEM resistance showed decreased susceptibility to IMP (40). Consistent with IMP mode of action, genes from the category of cell wall and membrane biogenesis were among those most highly represented in *E. coli* and *K. pneumoniae*. Amidases such as AmiC split the peptidoglycan (PG) of daughter cells during cell division (37). These amidases are autoinhibited and AmiC is activated by NlpD, a lipoprotein anchored in the outer membrane (31). Mutations in both *amiC* and *nlpD* contributed to a decrease in susceptibility to IMP (Table 5). It was demonstrated that the Tol-Pal system is implicated in regulating cell wall cleavage during cell division by activating NlpD (41) as well as in the modulation of PG synthesis (42). TolA, part of the Tol-Pal complex, was found mutated in three mutants of *E. coli*, and the M67I mutation decreased the susceptibility of the WT strain by 2-fold (Table 5). Mutations in *amiC*, *nlpD*, and *tolA* are likely to be loss-of-function mutations, since *nlpD* and *amiC* have nonsense mutations or InDels in many mutants (see Fig. S1A and B in the supplemental material). Our observations are consistent with previous studies where mutants lacking *nlpD* or amidases and several lytic transglycosylases (see below) displayed a delayed lysis response to ampicillin (43, 44).

The PG is made of alternating *N*-acetylglucosamine (GlcNAc) and *N*-acetylmuramic acid (MurNAc) connected by a β-1,4-glycosidic bond (37). Lytic transglycosylases (LTs) cleave this glycosidic bond (37). *E. coli* has eight membrane-bound LTs (MLTs) and one soluble LT named Slt70 (37). Several of these LTs (MltA, MltB, MltD, and RlpA) were mutated in single *E. coli* or *K. pneumoniae* mutants and were not studied (Tables S2 and S3), but the *yceG* (MltG) gene was mutated in 20 *E. coli* mutants, including 5 with nonsense mutations (Table 1). The transformation of the mutation Q92* in the *E. coli* ATCC 25922 WT did not change the susceptibility of the strain to IMP, and it did not provide a growth advantage in the presence of IMP (Table 5) (Fig. 4). While we could not find a specific role of *yceG* in IMP resistance, its frequent mutation in *E. coli* suggests a role possibly in combination with other mutations. Indeed, MltG was shown to interact with PBP1b and in the absence of PBP1b, MltG was shown to be toxic (45). Since IMP inhibits PBP1b, it is possible that loss-of-function mutations in *yceG* are selected to limit its toxicity. Inhibition of PBPs by β-lactams leads to an accumulation of non-cross-linked PG, and Slt70 is the main enzyme responsible for destroying this nascent PG (46). Slt inactivation produced differential effects on β-lactam sensitivity depending on the genetic background (46–48). Here, we showed that a *slt* nonsense mutation (R475*) in *E. coli* ATCC 25922 decreased the susceptibility to IMP by 2-fold.

The response of *P. aeruginosa* to IMP differed extensively from the responses seen with the two *Enterobacteriaceae* species. The outer membrane permeability of *P. aeruginosa* is about 12-to-100-fold lower than that of *E. coli* (49), and this is probably due to a reduced number of general diffusion porins and the presence of a variety of specific porins such as OprD (16, 50). IMP penetrates the pseudomonal membrane through OprD (51). Resistance to IMP in *P. aeruginosa* can occur through loss of OprD, which has been reported to take place at the levels of transcription and translation (14, 52). Mutations resulting in a premature stop codon were found in a number of clinical isolates (53–56), several of which (W6*, Q19*, W65*, W138*, Q158*, W277*, Q295*, W339*, and W415*) were also detected in this study together with new ones (Q30*, Q67*, Q79*, and Q235*) (Table 2). Stop codons occurred at tryptophan or glutamine residues, representing the only two codons that can be changed to a stop codon through a single transition (along with one of the six codons for arginine) induced by EMS. TCSs are known to downregulate OprD and contribute to IMP resistance (57, 58). Among the *P. aeruginosa* ATCC 27853 mutants selected in this study, 19 mutants had a mutation either in the sensor HK gene (A4W92_13070) or in the gene encoding its response regulator (A4W92_13065) without having a mutated *oprD* gene (Table 2). Two independent mutants had a mutation in another sensor HK gene (A4W92_04840) (Table 2). These mutated HKs belong to the same clade as the ones known to regulate OprD (59). Two mutations (E198K and Q258*) in the sensor HK PhoQ (A4W92_05675) were detected in two independent clones (Table 2). A PhoQ-null mutant is resistant to polymyxin B and to aminoglycoside antibiotics (60–62), and PhoQ mutants were reported in *P. aeruginosa* clinical isolates resistant to polymyxin B (63) or colistin (polymyxin E) (64). Current understanding would suggest that the mutated HKs activate their respective response regulators and that they in turn downregulate *oprD*. Mutated HKs were also observed in *E. coli* and *K. pneumoniae* strains resistant to IMP (Table S5), highlighting the potential key role of HKs in IMP responses in Gram-negative bacteria.

Our chemogenomic screen performed with three bacterial species highlighted shared and species-specific responses to IMP. The most highly mutated genes encoded proteins involved in transcription, signal transduction, and membrane/cell envelope biogenesis. The number of mutants investigated allowed a holistic view of the response to IMP and enabled concentrating our functional work on the most frequently recurrent genes. Most mutations tested in *E. coli* were associated with a 2-fold difference in IMP susceptibility. This relatively low level of resistance may reflect more-subtle roles for the mutations, such as facilitating resistance emergence or compensating for fitness cost. Many other mutations are likely to be involved in response to IMP, and our data set can be useful to better understand IMP and to find strategies to restore carbapenem susceptibility in Gram-negative bacteria.

MATERIALS AND METHODS

Bacterial strains, plasmids, and growth conditions. Bacterial strains and plasmids used in this study are listed in Table S8 in the supplemental material. Unless otherwise specified, *E. coli* (ATCC 25922), *K. pneumoniae* (ATCC 13883), and *P. aeruginosa* (ATCC 27853) were cultured on Luria-Bertani (LB) or nutrient agar (1.5%) and incubated at 37°C for 18 to 24 h. Liquid cultures were grown in LB for *E. coli* and in brain heart infusion (BHI) medium for *K. pneumoniae* and *P. aeruginosa*. Plasmid pRedET and the FRT-flanked PGK-gb2-kan cassette (catalogue number K006) and the enhanced FLP expression plasmid 707-FLPe (catalogue number A104) with a tetracycline resistance marker were obtained from Gene Bridges GmbH. IMP-monohydrate and MEM were purchased from Santa Cruz Biotechnology; all other chemicals were purchased from Sigma-Aldrich.

Antibacterial susceptibility testing. Analyses of the IMP or MEM MICs for the WT strain of each of the three species and for their respective mutants and optimization of the EMS concentrations (Table S8) were performed by microdilution in 96-well plates according to recommendations from the CLSI. The IMP or MEM MICs for the single or double knock-ins were determined by macrodilution. All MICs were determined from at least three independent biological replicates, each replicate being further assessed in technical duplicates.

Chemical mutagenesis and selection of antibiotic-resistant mutants. Optimization was performed by testing different concentrations of EMS equivalent to 4×, 8×, or 16× its MIC for each of the three species for either 10 or 20 min. We selected conditions that allowed treated cells to reach an optical density at 600 nm (OD$_{600}$) of 0.5 in less than 6 h. For *K. pneumoniae* and *P. aeruginosa*, this represented an EMS concentration equivalent to 4 times their MIC (0.024 g/ml and 0.012 g/ml, respectively) maintained for 10 min. For *E. coli*, we used an EMS concentration equivalent to 8 times its MIC (0.048 g/ml) maintained for 20 min. The minimum concentration of IMP used for selection was determined as the concentration at which growth occurred in the presence of IMP for the mutagenized populations but not for the nonmutagenized control populations. This represented IMP concentrations equivalent to 16× and 20× the MIC in the case of *E. coli* (4 and 5 μg/ml) and between 2× and 4× the MIC for both *K. pneumoniae* (2 and 4 μg/ml) and *P. aeruginosa* (4 and 8 μg/ml). No clones survived beyond these concentrations. The detailed protocol was as follows: the overnight (ON) cultures of the strains were diluted and incubated at 37°C with shaking (220 rpm) until they reached an OD$_{600}$ of 0.5. Each culture was separated into two tubes of 10 ml. We added EMS to one of the two tubes at the appropriate concentration. Cultures were incubated for 10 min (*K. pneumoniae* and *P. aeruginosa*) or 20 min (*E. coli*) at 37°C. Cultures were then diluted by half using ice-cold medium and then further diluted by 1/10 before being incubated until an OD$_{600}$ of 0.5 was reached. The cultures were centrifuged at 4,000 rpm for 5 min, and then the pellet was resuspended in 200 μl of the culture medium. Ten-fold dilutions (from 10^{-3} to 10^{-7}) were spread on agar plates to allow colony counting.

In order to select mutants resistant to IMP, 100-μl volumes of the mutagenized cultures were spread on agar plates containing an increasing concentration of the antibiotic (between 2× and 20× the MIC depending on the species). Agar plates were incubated overnight at 37°C, and colonies were counted the next day. This protocol was performed for each strain in duplicate.

Extraction and quantification of DNA. Genomic DNA (gDNA) was extracted using a Wizard Genomic DNA purification kit (Promega) according to the manufacturer's protocol. The purity of the gDNA was analyzed using a NanoDrop spectrophotometer. Quantification was performed by fluorescence detection using a QuantiFluor One double-stranded DNA (dsDNA) system (Promega).

DNA sequencing. Libraries were produced from 0.8 ng of gDNA using a Nextera XT DNA Library Prep kit (Illumina) according to the manufacturer's protocol. Libraries were verified by the use of model 2100 Bioanalyzer high-sensitivity DNA chips (Agilent) and quantified by the use of a QuantiFluor One dsDNA system (Promega). Libraries were sequenced on an Illumina HiSeq 2500 system (101-nt paired-end sequencing) at a final concentration of 8 pM.

Mut-Seq data analysis. Sequence reads were aligned to the *E. coli* ATCC 25922 (BioProject accession no. PRJNA244551), *K. pneumoniae* ATCC 13883 (PRJNA244567), and *P. aeruginosa* ATCC 27853 (PRJNA316664) genomes using bwa-mem software (65). The seed length was 32, and 2 mismatches were allowed within the seed; the maximum number of mismatches allowed was 4. Read duplicates were marked using Picard (http://broadinstitute.github.io/picard/), and calling of SNVs and InDels was done using GATK software (66). Mutations in common with the WT strain sequence examined in parallel were excluded, and the remaining mutations (i.e., mutant-specific mutations) were annotated. To ease the comparisons among the three species, the common COGs (30) were determined using the workflow of COGsoft (https://sourceforge.net/projects/cogtriangles/files/).

Generation of knock-ins in *E. coli*. We first transformed *E. coli* ATCC 25922 with the expression plasmid pRedET as recommended by the manufacturer (Gene Bridges GmbH). Mutated PCR fragments of the genes of interest were amplified from the appropriate *E. coli* mutant and fused to the FRT-flanked PGK-gb2-kan cassette before being transformed in the *E. coli* strain containing the pRedEt plasmid. This strategy was previously described by Sukhija et al. and Pyne et al. (67, 68). L-Arabinose was added to induce the expression of the Red/ET recombination proteins, and transformants were selected with Kan (40 μg/ml). Colonies were analyzed by colony PCR and sequencing. All primers used to generate the single knock-ins and to check the right integration of the gene replacement cassette are listed in Table S8. The enhanced FLP conditional expression plasmid 707-FLPe was transformed into the strain containing the gene replacement cassette so that recombination would occur at the FRT sites. PCR was used to confirm both the removal of the Kan cassette by FLP recombination and the presence of the knock-in mutation.

Testing the effect of mutations on the growth of *E. coli*. Cultures (OD_{600} = 0.9) were serially diluted (10^{-1} to 10^{-6}) in LB, and 5-μl volumes were spotted on freshly prepared LB agar plates supplemented with different concentrations of IMP. Plates were incubated at 37°C overnight, and they were photographed the next day using an AlphaImager system (Alpha Innotech).

For determination of the growth curve in liquid medium, 5 μl of 1×10^7 CFU/ml was inoculated in 200 μl of LB medium in the absence or presence of IMP at concentrations of 0.03 to 4 μg/ml in 96-well plates. The plate was incubated at 37°C, and the OD_{600} was read each 30 min after shaking for 10 s using a Cytation 5 multimode reader. Each assay was done in technical triplicate and biological triplicate.

Data availability. The WGS data have been deposited in the SRA database, and the accession numbers are listed in Table S9.

SUPPLEMENTAL MATERIAL

Supplemental material for this article may be found at https://doi.org/10.1128/mSystems.00465-19.

FIG S1, TIF file, 0.8 MB.
TABLE S1, PDF file, 0.1 MB.
TABLE S2, XLSX file, 0.4 MB.
TABLE S3, XLSX file, 0.1 MB.
TABLE S4, XLSX file, 0.1 MB.
TABLE S5, XLSX file, 0.03 MB.
TABLE S6, XLSX file, 0.1 MB.
TABLE S7, XLSX file, 0.02 MB.
TABLE S8, PDF file, 0.03 MB.
TABLE S9, XLSX file, 0.02 MB.

REFERENCES

1. Tacconelli E, Carrara E, Savoldi A, Harbarth S, Mendelson M, Monnet DL, Pulcini C, Kahlmeter G, Kluytmans J, Carmeli Y, Ouellette M, Outterson K, Patel J, Cavaleri M, Cox EM, Houchens CR, Grayson ML, Hansen P, Singh N, Theuretzbacher U, Magrini N. 2018. Discovery, research, and development of new antibiotics: the WHO priority list of antibiotic-resistant bacteria and tuberculosis. Lancet Infect Dis 18:318–327. https://doi.org/10.1016/S1473-3099(17)30753-3.
2. Nordmann P, Dortet L, Poirel L. 2012. Carbapenem resistance in *Enterobacteriaceae*: here is the storm! Trends Mol Med 18:263–272. https://doi.org/10.1016/j.molmed.2012.03.003.
3. Navon-Venezia S, Kondratyeva K, Carattoli A. 2017. Klebsiella pneumoniae: a major worldwide source and shuttle for antibiotic resistance. FEMS Microbiol Rev 41:252–275. https://doi.org/10.1093/femsre/fux013.
4. López-Causapé C, Cabot G, Del Barrio-Tofiño E, Oliver A. 2018. The versatile mutational resistome of *Pseudomonas aeruginosa*. Front Microbiol 9:685. https://doi.org/10.3389/fmicb.2018.00685.
5. Peleg AY, Hooper DC. 2010. Hospital-acquired infections due to gram-negative bacteria. N Engl J Med 362:1804–1813. https://doi.org/10.1056/NEJMra0904124.
6. Papp-Wallace KM, Endimiani A, Taracila MA, Bonomo RA. 2011. Carbapenems: past, present, and future. Antimicrob Agents Chemother 55:4943–4960. https://doi.org/10.1128/AAC.00296-11.
7. Lob SH, Hackel MA, Kazmierczak KM, Young K, Motyl MR, Karlowsky JA, Sahm DF. 24 May 2017, posting date. In vitro activity of imipenem-relebactam against Gram-negative ESKAPE pathogens isolated by clinical laboratories in the United States in 2015 (results from the SMART Global Surveillance Program). Antimicrob Agents Chemother https://doi.org/10.1128/AAC.02209-16.
8. Diene SM, Rolain JM. 2014. Carbapenemase genes and genetic platforms in Gram-negative bacilli: *Enterobacteriaceae*, *Pseudomonas*, and *Acinetobacter* species. Clin Microbiol Infect 20:831–838. https://doi.org/10.1111/1469-0691.12655.
9. Bidet P, Burghoffer B, Gautier V, Brahimi N, Mariani-Kurkdjian P, El-Ghoneimi A, Bingen E, Arlet G. 2005. In vivo transfer of plasmid-encoded ACC-1 AmpC from *Klebsiella pneumoniae* to *Escherichia coli* in an infant and selection of impermeability to imipenem in K. pneumoniae. Antimicrob Agents Chemother 49:3562–3565. https://doi.org/10.1128/AAC.49.8.3562-3565.2005.
10. Queenan AM, Bush K. 2007. Carbapenemases: the versatile beta-lactamases. Clin Microbiol Rev 20:440–458. https://doi.org/10.1128/CMR.00001-07.
11. Chia JH, Siu LK, Su LH, Lin HS, Kuo AJ, Lee MH, Wu TL. 2009. Emergence of carbapenem-resistant *Escherichia coli* in Taiwan: resistance due to combined CMY-2 production and porin deficiency. J Chemother 21:621–626. https://doi.org/10.1179/joc.2009.21.6.621.
12. Shin SY, Bae IK, Kim J, Jeong SH, Yong D, Kim JM, Lee K. 2012. Resistance to carbapenems in sequence type 11 *Klebsiella pneumoniae* is related to DHA-1 and loss of OmpK35 and/or OmpK36. J Med Microbiol 61:239–245. https://doi.org/10.1099/jmm.0.037036-0.
13. Rodriguez-Martinez JM, Poirel L, Nordmann P. 2009. Molecular epidemiology and mechanisms of carbapenem resistance in *Pseudomonas aeruginosa*. Antimicrob Agents Chemother 53:4783–4788. https://doi.org/10.1128/AAC.00574-09.

14. Fang ZL, Zhang LY, Huang YM, Qing Y, Cao KY, Tian GB, Huang X. 2014. OprD mutations and inactivation in imipenem-resistant *Pseudomonas aeruginosa* isolates from China. Infect Genet Evol 21:124–128. https://doi.org/10.1016/j.meegid.2013.10.027.

15. Hong DJ, Bae IK, Jang IH, Jeong SH, Kang HK, Lee K. 2015. Epidemiology and characteristics of metallo-beta-lactamase-producing *Pseudomonas aeruginosa*. Infect Chemother 47:81–97. https://doi.org/10.3947/ic.2015.47.2.81.

16. Pang Z, Raudonis R, Glick BR, Lin TJ, Cheng Z. 2019. Antibiotic resistance in *Pseudomonas aeruginosa*: mechanisms and alternative therapeutic strategies. Biotechnol Adv 37:177–192. https://doi.org/10.1016/j.biotechadv.2018.11.013.

17. Zhanel GG, Lawrence CK, Adam H, Schweizer F, Zelenitsky S, Zhanel M, Lagace-Wiens PRS, Walkty A, Denisuik A, Golden A, Gin AS, Hoban DJ, Lynch JP, III, Karlowsky JA. 2018. Imipenem-relebactam and meropenem-vaborbactam: two novel carbapenem-beta-lactamase inhibitor combinations. Drugs 78:65–98. https://doi.org/10.1007/s40265-017-0851-9.

18. Schmidt-Malan SM, Mishra AJ, Mushtaq A, Brinkman CL, Patel R. 27 July 2018, posting date. In vitro activity of imipenem-relebactam and ceftolozane-tazobactam against resistant Gram-negative bacilli. Antimicrob Agents Chemother https://doi.org/10.1128/AAC.00533-18.

19. Livermore DM, Yang YJ. 1989. Comparative activity of meropenem against *Pseudomonas aeruginosa* strains with well-characterized resistance mechanisms. J Antimicrob Chemother 24(Suppl A):149–159. https://doi.org/10.1093/jac/24.suppl_a.149.

20. Voutsinas D, Mavroudis T, Avlamis A, Giamarellou H. 1989. In-vitro activity of meropenem, a new carbapenem, against multiresistant *Pseudomonas aeruginosa* compared with that of other antipseudomonal antimicrobials. J Antimicrob Chemother 24(Suppl A):143–147. https://doi.org/10.1093/jac/24.suppl_a.143.

21. Feng J, Lupien A, Gingras H, Wasserscheid J, Dewar K, Legare D, Ouellette M. 2009. Genome sequencing of linezolid-resistant *Streptococcus pneumoniae* mutants reveals novel mechanisms of resistance. Genome Res 19:1214–1223. https://doi.org/10.1101/gr.089342.108.

22. Fani F, Leprohon P, Legare D, Ouellette M. 2011. Whole genome sequencing of penicillin-resistant *Streptococcus pneumoniae* reveals mutations in penicillin-binding proteins and in a putative iron permease. Genome Biol 12:R115. https://doi.org/10.1186/gb-2011-12-11-r115.

23. Koser CU, Ellington MJ, Peacock SJ. 2014. Whole-genome sequencing to control antimicrobial resistance. Trends Genet 30:401–407. https://doi.org/10.1016/j.tig.2014.07.003.

24. Rimoldi SG, Gentile B, Pagani C, Di Gregorio A, Anselmo A, Palozzi AM, Fortunato A, Pittiglio V, Ridolfo AL, Gismondo MR, Rizzardini G, Lista F. 2017. Whole genome sequencing for the molecular characterization of carbapenem-resistant *Klebsiella pneumoniae* strains isolated at the Italian ASST Fatebenefratelli Sacco Hospital, 2012–2014. BMC Infect Dis 17:666. https://doi.org/10.1186/s12879-017-2760-7.

25. Robins WP, Faruque SM, Mekalanos JJ. 2013. Coupling mutagenesis and parallel deep sequencing to probe essential residues in a genome or gene. Proc Natl Acad Sci U S A 110:E848–E857. https://doi.org/10.1073/pnas.1222538110.

26. Gingras H, Patron K, Bhattacharya A, Leprohon P, Ouellette M. 25 April 2019, posting date. Gain and loss of function screens coupled to next generation sequencing for antibiotic mode of action and resistance studies in *Streptococcus pneumoniae*. Antimicrob Agents Chemother https://doi.org/10.1128/AAC.02381-18.

27. Brammeld JS, Petljak M, Martincorena I, Williams SP, Alonso LG, Dalmases A, Bellosillo B, Robles-Espinoza CD, Price S, Barthorpe S, Tarpey P, Alifrangis C, Bignell G, Vidal J, Young J, Stebbings L, Beal K, Stratton MR, Saez-Rodriguez J, Garnett M, Montagut C, Iorio F, McDermott U. 2017. Genome-wide chemical mutagenesis screens allow unbiased saturation of the cancer genome and identification of drug resistance mutations. Genome Res 27:613–625. https://doi.org/10.1101/gr.213546.116.

28. Wayne P. 2019. CLSI. Performance Standards for Antimicrobial Susceptibility Testing. 29th ed. CLSI supplement M100. Clinical and Laboratory Standards Institute, Wayne, PA.

29. Du H, Pan B, Chen T. 2017. Evaluation of chemical mutagenicity using next generation sequencing: a review. J Environ Sci Health C Environ Carcinog Ecotoxicol Rev 35:140–158. https://doi.org/10.1080/10590501.2017.1328831.

30. Galperin MY, Makarova KS, Wolf YI, Koonin EV. 2015. Expanded microbial genome coverage and improved protein family annotation in the COG database. Nucleic Acids Res 43:D261–D269. https://doi.org/10.1093/nar/gku1223.

31. Peters NT, Dinh T, Bernhardt TG. 2011. A fail-safe mechanism in the septal ring assembly pathway generated by the sequential recruitment of cell separation amidases and their activators. J Bacteriol 193:4973–4983. https://doi.org/10.1128/JB.00316-11.

32. Lehrbach NJ, Ji F, Sadreyev R. 2017. Next-generation sequencing for identification of EMS-induced mutations in *Caenorhabditis elegans*. Curr Protoc Mol Biol 117:7.29.1–7 29.12. https://doi.org/10.1002/cpmb.27.

33. Borukhov S, Nudler E. 2008. RNA polymerase: the vehicle of transcription. Trends Microbiol 16:126–134. https://doi.org/10.1016/j.tim.2007.12.006.

34. Campbell EA, Muzzin O, Chlenov M, Sun JL, Olson CA, Weinman O, Trester-Zedlitz ML, Darst SA. 2002. Structure of the bacterial RNA polymerase promoter specificity sigma subunit. Mol Cell 9:527–539. https://doi.org/10.1016/s1097-2765(02)00470-7.

35. Paget MS. 2015. Bacterial sigma factors and anti-sigma factors: structure, function and distribution. Biomolecules 5:1245–1265. https://doi.org/10.3390/biom5031245.

36. Sauvage E, Terrak M. 17 February 2016, posting date. Glycosyltransferases and transpeptidases/penicillin-binding proteins: valuable targets for new antibacterials. Antibiotics (Basel) https://doi.org/10.3390/antibiotics5010012.

37. Dik DA, Fisher JF, Mobashery S. 2018. Cell-wall recycling of the Gram-negative bacteria and the nexus to antibiotic resistance. Chem Rev 118:5952–5984. https://doi.org/10.1021/acs.chemrev.8b00277.

38. Rodloff AC, Goldstein EJ, Torres A. 2006. Two decades of imipenem therapy. J Antimicrob Chemother 58:916–929. https://doi.org/10.1093/jac/dkl354.

39. Edwards JR, Turner PJ. 1995. Laboratory data which differentiate meropenem and imipenem. Scand J Infect Dis Suppl 96:5–10.

40. Adler M, Anjum M, Andersson DI, Sandegren L. 2016. Combinations of mutations in envZ, ftsI, mrdA, acrB and acrR can cause high-level carbapenem resistance in *Escherichia coli*. J Antimicrob Chemother 71:1188–1198. https://doi.org/10.1093/jac/dkv475.

41. Tsang MJ, Yakhnina AA, Bernhardt TG. 2017. NlpD links cell wall remodeling and outer membrane invagination during cytokinesis in *Escherichia coli*. PLoS Genet 13:e1006888. https://doi.org/10.1371/journal.pgen.1006888.

42. Gray AN, Egan AJ, van't Veer IL, Verheul J, Colavin A, Koumoutsi A, Biboy J, Altelaar AFM, Damen MJ, Huang KC, Simorre J-P, Breukink E, den Blaauwen T, Typas A, Gross CA, Vollmer W. 7 May 2015, posting date. Coordination of peptidoglycan synthesis and outer membrane constriction during *Escherichia coli* cell division. Elife https://doi.org/10.7554/eLife.07118.

43. Heidrich C, Ursinus A, Berger J, Schwarz H, Holtje JV. 2002. Effects of multiple deletions of murein hydrolases on viability, septum cleavage, and sensitivity to large toxic molecules in *Escherichia coli*. J Bacteriol 184:6093–6099. https://doi.org/10.1128/jb.184.22.6093-6099.2002.

44. Uehara T, Dinh T, Bernhardt TG. 2009. LytM-domain factors are required for daughter cell separation and rapid ampicillin-induced lysis in *Escherichia coli*. J Bacteriol 191:5094–5107. https://doi.org/10.1128/JB.00505-09.

45. Yunck R, Cho H, Bernhardt TG. 2016. Identification of MltG as a potential terminase for peptidoglycan polymerization in bacteria. Mol Microbiol 99:700–718. https://doi.org/10.1111/mmi.13258.

46. Cho H, Uehara T, Bernhardt TG. 2014. Beta-lactam antibiotics induce a lethal malfunctioning of the bacterial cell wall synthesis machinery. Cell 159:1300–1311. https://doi.org/10.1016/j.cell.2014.11.017.

47. Templin MF, Edwards DH, Holtje JV. 1992. A murein hydrolase is the specific target of bulgecin in *Escherichia coli*. J Biol Chem 267:20039–20043.

48. Costa CS, Anton DN. 2006. High-level resistance to mecillinam produced by inactivation of soluble lytic transglycosylase in *Salmonella enterica* serovar Typhimurium. FEMS Microbiol Lett 256:311–317. https://doi.org/10.1111/j.1574-6968.2006.00133.x.

49. Hancock RE. 1998. Resistance mechanisms in *Pseudomonas aeruginosa* and other nonfermentative gram-negative bacteria. Clin Infect Dis 27(Suppl 1):S93–S99. https://doi.org/10.1086/514909.

50. Hancock RE, Brinkman FS. 2002. Function of pseudomonas porins in uptake and efflux. Annu Rev Microbiol 56:17–38. https://doi.org/10.1146/annurev.micro.56.012302.160310.

51. Trias J, Nikaido H. 1990. Outer membrane protein D2 catalyzes facilitated diffusion of carbapenems and penems through the outer membrane

of *Pseudomonas aeruginosa*. Antimicrob Agents Chemother 34:52–57. https://doi.org/10.1128/aac.34.1.52.

52. Shu JC, Kuo AJ, Su LH, Liu TP, Lee MH, Su IN, Wu TL. 2017. Development of carbapenem resistance in *Pseudomonas aeruginosa* is associated with OprD polymorphisms, particularly the amino acid substitution at codon 170. J Antimicrob Chemother 72:2489–2495. https://doi.org/10.1093/jac/dkx158.

53. Pirnay JP, De Vos D, Mossialos D, Vanderkelen A, Cornelis P, Zizi M. 2002. Analysis of the *Pseudomonas aeruginosa* oprD gene from clinical and environmental isolates. Environ Microbiol 4:872–882. https://doi.org/10.1046/j.1462-2920.2002.00281.x.

54. Gutierrez O, Juan C, Cercenado E, Navarro F, Bouza E, Coll P, Perez JL, Oliver A. 2007. Molecular epidemiology and mechanisms of carbapenem resistance in *Pseudomonas aeruginosa* isolates from Spanish hospitals. Antimicrob Agents Chemother 51:4329–4335. https://doi.org/10.1128/AAC.00810-07.

55. Kao CY, Chen SS, Hung KH, Wu HM, Hsueh PR, Yan JJ, Wu JJ. 2016. Overproduction of active efflux pump and variations of OprD dominate in imipenem-resistant *Pseudomonas aeruginosa* isolated from patients with bloodstream infections in Taiwan. BMC Microbiol 16:107. https://doi.org/10.1186/s12866-016-0719-2.

56. Courtois N, Caspar Y, Maurin M. 2018. Phenotypic and genetic resistance traits of *Pseudomonas aeruginosa* strains infecting cystic fibrosis patients: a French cohort study. Int J Antimicrob Agents 52:358–364. https://doi.org/10.1016/j.ijantimicag.2018.05.008.

57. Perron K, Caille O, Rossier C, Van Delden C, Dumas J-L, Köhler T. 2004. CzcR-CzcS, a two-component system involved in heavy metal and carbapenem resistance in *Pseudomonas aeruginosa*. J Biol Chem 279: 8761–8768. https://doi.org/10.1074/jbc.M312080200.

58. Caille O, Rossier C, Perron K. 2007. A copper-activated two-component system interacts with zinc and imipenem resistance in *Pseudomonas aeruginosa*. J Bacteriol 189:4561–4568. https://doi.org/10.1128/JB.00095-07.

59. Chen YT, Chang HY, Lu CL, Peng HL. 2004. Evolutionary analysis of the two-component systems in *Pseudomonas aeruginosa* PAO1. J Mol Evol 59:725–737. https://doi.org/10.1007/s00239-004-2663-2.

60. Macfarlane EL, Kwasnicka A, Ochs MM, Hancock RE. 1999. PhoP-PhoQ homologues in *Pseudomonas aeruginosa* regulate expression of the outer-membrane protein OprH and polymyxin B resistance. Mol Microbiol 34:305–316. https://doi.org/10.1046/j.1365-2958.1999.01600.x.

61. Macfarlane EL, Kwasnicka A, Hancock RE. 2000. Role of *Pseudomonas aeruginosa* PhoP-phoQ in resistance to antimicrobial cationic peptides and aminoglycosides. Microbiology 146:2543–2554. https://doi.org/10.1099/00221287-146-10-2543.

62. Gooderham WJ, Hancock RE. 2009. Regulation of virulence and antibiotic resistance by two-component regulatory systems in *Pseudomonas aeruginosa*. FEMS Microbiol Rev 33:279–294. https://doi.org/10.1111/j.1574-6976.2008.00135.x.

63. Barrow K, Kwon DH. 2009. Alterations in two-component regulatory systems of phoPQ and pmrAB are associated with polymyxin B resistance in clinical isolates of *Pseudomonas aeruginosa*. Antimicrob Agents Chemother 53:5150–5154. https://doi.org/10.1128/AAC.00893-09.

64. Miller AK, Brannon MK, Stevens L, Johansen HK, Selgrade SE, Miller SI, Hoiby N, Moskowitz SM. 2011. PhoQ mutations promote lipid A modification and polymyxin resistance of *Pseudomonas aeruginosa* found in colistin-treated cystic fibrosis patients. Antimicrob Agents Chemother 55:5761–5769. https://doi.org/10.1128/AAC.05391-11.

65. Li H, Durbin R. 2009. Fast and accurate short read alignment with Burrows-Wheeler transform. Bioinformatics 25:1754–1760. https://doi.org/10.1093/bioinformatics/btp324.

66. McKenna A, Hanna M, Banks E, Sivachenko A, Cibulskis K, Kernytsky A, Garimella K, Altshuler D, Gabriel S, Daly M, DePristo MA. 2010. The Genome Analysis Toolkit: a MapReduce framework for analyzing next-generation DNA sequencing data. Genome Res 20:1297–1303. https://doi.org/10.1101/gr.107524.110.

67. Pyne ME, Moo-Young M, Chung DA, Chou CP. 2015. Coupling the CRISPR/Cas9 system with lambda red recombineering enables simplified chromosomal gene replacement in *Escherichia coli*. Appl Environ Microbiol 81:5103–5114. https://doi.org/10.1128/AEM.01248-15.

68. Sukhija K, Pyne M, Ali S, Orr V, Abedi D, Moo-Young M, Chou CP. 2012. Developing an extended genomic engineering approach based on recombineering to knock-in heterologous genes to *Escherichia coli* genome. Mol Biotechnol 51:109–118. https://doi.org/10.1007/s12033-011-9442-2.